Electric Power Systems Research 211 (2022) 108448

Contents lists available at ScienceDirect

Electric Power Systems Research

journal homepage: www.elsevier.com/locate/epsr

Investigating small-disturbance stability in power systems with grid-following and grid-forming VSCs using hybrid modelling approaches

Youhong Chen [a,*], Luke Benedetti [b], Robin Preece [a], Panagiotis N. Papadopoulos [b], Mike Barnes [a], Agustí Egea-Àlvarez [b]

[a] Department of Electrical and Electronic Engineering, The University of Manchester, Manchester, UK
[b] Department of Electronic and Electrical Engineering, University of Strathclyde, Glasgow, UK

ARTICLE INFO

Keywords:
Hybrid model
Small-signal stability
VSC
Grid-forming
Grid-following

ABSTRACT

The mass integration of power electronics-based devices is changing small-disturbance stability issues in power systems from primarily interactions between synchronous generators to include interactions between power electronic devices and the AC network. However, modelling of AC networks for small-disturbance stability assessment in large power systems generally do not include the transmission network dynamics and, therefore, fails to identify these newly emerging power phenomena. A suggested solution is the hybrid modelling approach which models the vicinity around the power electronics with network dynamics while representing the remainder of the network with a steady-state model. This paper identifies the most appropriate selection of dynamic AC network modelling in accordance with different scenarios including different power electronic control schemes, different power electronic operation modes, and different locations of power electronic devices. It is shown that more of the network must be modelled dynamically when VSCs are located in low SCR regions, operating in inverting mode, and using grid following or grid-forming control with inner current control explicitly modelled. Contrastingly, less dynamic detail is required for high SCR regions, rectifying mode, and when modelling grid forming control without explicit representation of the inner current controllers. Investigations are performed using the IEEE 39-bus test system.

1. Introduction

Traditional small-disturbance stability analysis of large power systems has focused on low-damped electromechanical oscillations involving synchronous generators (SGs), such as improving the damping of inter-area oscillatory modes [1]. Since these oscillatory modes are usually located in low-frequency ranges, the analysis typically makes use of a network model which consists of algebraic equations, neglecting the fast electromagnetic dynamics of the transmission lines. This is possible due to the principle of time-scale separation [2]. However, the integration of large-scale renewable energy sources (RES) through power electronics based (PEB) devices is expected to proliferate in future power systems. The issues caused by the interactions between PEB devices and the AC network, combined with other converter-driven stability issues, have attracted increasing attention [3]. This is partly driven by the high bandwidth of voltage source converters (VSCs) operating with grid following (GFL) control schemes. The fast control action of these devices can interact with the electromagnetic dynamics of the grid [4]. The conventional modelling of networks with algebraic equations fails to capture these fast dynamics and, therefore, cannot identify new emerging system stability issues. Existing research [2,5] has revealed that steady-state network modelling can cause system stability determination errors, which become evident when compared with results from AC network dynamic modelling via ordinary differential equations (ODEs).

A hybrid modelling approach proposed in [6] provides a potential solution for small-disturbance stability analysis in large systems. The AC network in the vicinity of power electronic interfaced generation is modelled with ODEs while the rest of the network is represented with algebraic equations. This brings the benefit of significantly reducing the order of the system while maintaining information on the electromagnetic grid elements which are expected to influence power system dynamics in high-RES penetration scenarios. However, no previous works have systematically investigated the selection of the ODE-represented

* Corresponding author.
E-mail address: youhong.chen@manchester.ac.uk (Y. Chen).

https://doi.org/10.1016/j.epsr.2022.108448
Received 5 October 2021; Received in revised form 14 April 2022; Accepted 2 July 2022
Available online 13 July 2022

AC network region with consideration of different VSC control schemes (grid forming and grid following), the VSC operation mode (rectifying or inverting), and the impact this has on stability assessment accuracy.

This paper establishes how stability assessment accuracy changes as the network region modelled using ODEs is varied. The investigation performed follows a similar procedure to [7] which investigates the impact of GFL VSCs on the hybrid modelling. However, the damping error used in [7] for determining the difference between models, may result in potentially misleading conclusions. Additionally, the work in [7] did excellent work in highlighting the need of hybrid modelling with GFL control but the procedure performed is very network specific and a thorough and detailed comparison procedure between models is not provided for practitioners. Hence, this paper develops a quantitative comparison methodology between different network models using a correlation based analysis of participation factors to assess the small signal stability assessment accuracy. Based on the developed methodology, this paper furthers the analysis of the locational impact of VSCs on grid dynamics with the introduction of a new generalized metric, more appropriate for assessing the impact of the dynamic network area included in hybrid models. The procedure is discussed in more detail in Section III.

With the aid of the proposed metric, the work is continued with an analysis of the impact that grid forming (GFM) controlled VSCs have on the selection of network region modelled dynamically. The potential interaction of GFM controllers and transmission line dynamics, despite the comparatively slow acting mechanisms in GFMs, has been highlighted in [8]. However, this was specifically for the Dispatchable Virtual Oscillator Control scheme whereas this paper investigates the Virtual Synchronous Machine (VSM) [9].

To summarize, the contributions of this paper are:

- A novel model comparison methodology for determining hybrid model sufficiency.
- An analysis of the impact of inverting mode and rectifying mode VSCs on control-network interactions.
- A comparison of GFL and GFM control on the hybrid modelling required.

2. Modelling

All modelling in this work has been completed in Matlab 2020a. This section discusses the modelling approach employed and the details of the power system elements included.

2.1. SG & VSC Modelling

Firstly, the SG and VSC are represented using ODEs. Small signal models are employed, with the derivation procedure detailed in [1]. The concept involves linearizing around the operating point being studied. This results in a model which is relevant for small deviations and allows for linear analysis techniques such as the investigation of eigenvalues.

SG Model: A 4th order SG model [10] is used with an IEEE DC1A excitor/AVR [11] which has a further three states.

VSC Specific Components: All VSCs have an RL filter impedance, measurement filters and a PWM first order time delay approximation. For more details, including the values used, see [12]. The converter in this paper uses an averaged model, neglecting switching effects [13].

GFL VSC Model: The GFL control scheme is the ubiquitous vector current control (VCC) which is operating on a voltage source converter (VSC). There are two main control loops within the VCC with the first being the inner current control loop which provides a voltage vector output through controlling the d and q currents. Within this loop, the currents are decoupled to allow the second (outer) control loop to synthesize the current references whilst maintaining the independent control of the active power and voltage magnitude [13]. The control parameters of the GFL used in this study are tuned to ensure stability at all locations with values from [12].

GFM VSC Model: The most frequently adopted GFM control scheme in the literature is the VSM. The term VSM can cover a wide range of implementations which share the aim of emulating the characteristics of an SG to differing levels of detail [9]. The VSM adopted in this research is based on the swing equation [1,14]. Besides the active power controller (APC) which creates the virtual rotor angle, a GFM requires a controller to maintain the synthesized voltage magnitude. A PI controller is adopted for this purpose, although a common alternative is the use of a reactive power-voltage droop [2,14]. A virtual inductance is included to emulate the voltage drop presented in a SM due to the stator [15]. Following this, a current reference is determined which is then supplied to the inner current controller. The general structure of the GFM controlled VSC used in this work is displayed in Fig. 1.

An alternative current limitation approach is to use the threshold induced virtual impedance current limiting technique in [16]. However, this has no impact on the small signal dynamics, provided the initial operating point is sufficiently below the current limit threshold. If this was implemented, Fig. 1 would not contain the inner controllers section. Both approaches are investigated in this work.

2.2. Steady-state network modelling

Within the steady-state network model, the dynamics of the network are neglected and represented by algebraic equations based on system admittance matrix, as is shown in (1).

$$i_{bus} = Y v_{bus} \tag{1}$$

In (1), i_{bus} is the injection currents at buses; v_{bus} is the vector of bus voltage; Y represents the system admittance matrix. The loads are modelled as self-admittances of the connected bus and added to the Y matrix.

2.3. Small-signal network modelling

When modeling the small-signal (dynamic) part of the network, the transmission line is implemented with the common PI model. This model is appropriate for the system studied and is also deemed appropriate for representing dynamics of the frequency of interest considering the prospective converter controller interactions [7]. The equations that represent the dynamics of the network lines are shown in (2) and (3).

$$\frac{di_L}{dt} = \frac{\omega}{L} v_s - \frac{\omega}{L} v_r - \frac{\omega R}{L} i_L - j\omega i_L \tag{2}$$

$$\frac{dv_{bus}}{dt} = \frac{\omega}{C} \sum i_L - j\omega v_{bus} \tag{3}$$

In (2) and (3), i_L is the current in the transmission line; v_{bus} is the bus voltage; ω represents the system frequency; v_s, v_r represent the sending-end and receiving-end of voltage of the transmission line respectively; R, L, C are the line resistance, inductance and capacitance respectively.

All loads are modelled as constant impedances. Inductive loads are represented as series RL impedances and capacitive loads are implemented as parallel RC impedances, to allow for the amalgamation of capacitive elements at each bus for the purposes of dynamic modelling consistency. The form of the dynamic equations for the loads will be the same as for the transmission lines shown in (2) and (3). The values of the impedances are determined from the active and reactive power of the loads at the operating points of interest.

2.4. Hybrid Modelling

As described previously, the hybrid model being discussed incorporates a mixture of algebraic and ODE representations for the grid dynamics. The working assumption is that the adjacent grid dynamics to the VSC location will have the most interactions with the controller and

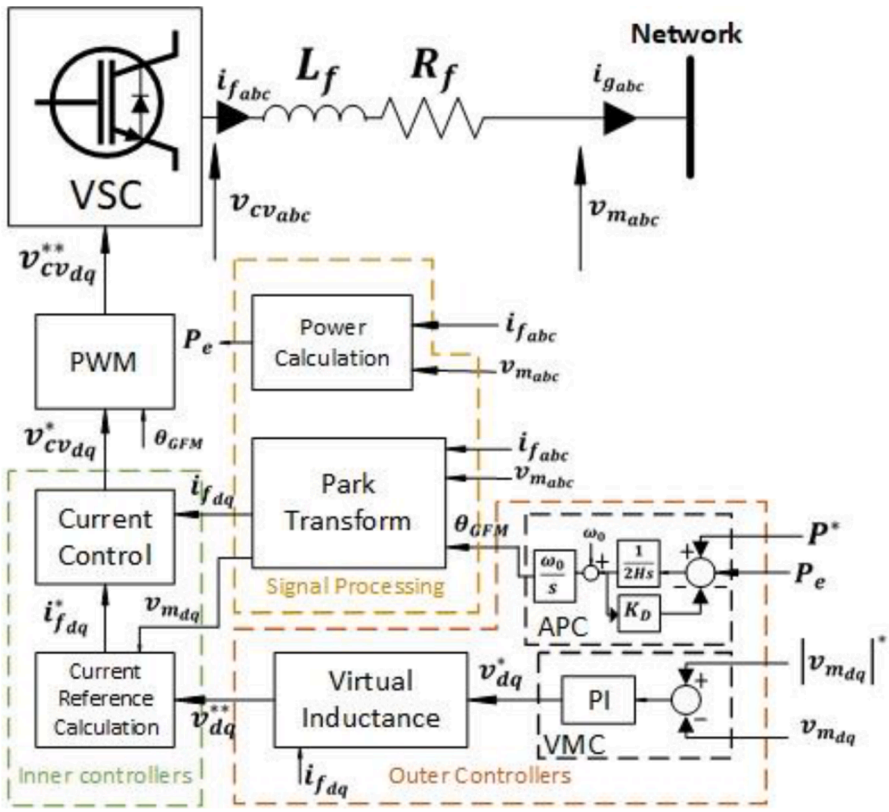

Fig. 1. Generic structure of GFM controlled VSC utilised in this work.

hence the part of the network closest to the VSC is considered as the dynamic area and is modelled with ODEs. The rest of network, meanwhile, is modelled with algebraic equations. The complete model that combines steady-state and dynamic parts is shown in (4).

$$\dot{x}_{dyn} = A_{dyn}x_{dyn} + B_{dyn}[v_{bou}]$$

$$i_{bou} = C_{dyn}x_{dyn}$$

$$i_{bus\&bou} = Yv_{bus\&bou} \tag{4}$$

In (4), x_{dyn} is the vector of state variables within the dynamic part of system; v_{bou} is the vector of bus voltages that are located at the boundary between the steady-state and dynamic parts of the network; i_{bou} represents the vector of interconnected currents between these two parts; $i_{bus\&bou}$ is the vector of injection currents that includes injection currents within both the steady-state network area and at the boundary; $v_{bus\&bou}$ represents the bus voltages within the steady-state part and at the boundary. As is shown in (4), the output of the dynamically modeled region, that is the interconnected current, is the input of the steady-state part of network. Similarly, the steady-state part of the network provides the bus voltages at the boundary and feeds these into the dynamic part of system. Consequently, the completed model is built by integrating the dynamic area of the network with the steady-state part of the network.

3. Methodology

This section presents the methodology to quantitatively compare dynamic results from different types of models (steady-state, and different orders of hybrid modelling) with the full dynamic model in order to assess the area of the network which should be modelled dynamically. The devised method identifies similar eigenvalue matches from different models based on a correlation-based assessment according to participation factor analysis. The developed methodology consists of three steps: identifying the key eigenvalues which represent VSC-network interactions; matching the key eigenvalues from reduced order models with the full dynamic model; and quantifying the error between the resulting matched key eigenvalues. The proposed comparison procedure is developed within MATLAB 2020.

3.1. Identifying the key eigenvalues

The initial step in the proposed methodology is to determine the eigenvalues of interest from the different models. The principal motivation behind developing this hybrid model is to capture interactions between VSCs and the network. Accordingly, the eigenvalues representing these power system dynamics will be determined and selected, as presented in (5).

$$x_i \epsilon X_{key} | x_i \epsilon X_{VSC} \cup X_{net} \tag{5}$$

In (5), x_i is the state variables of eigenvalue λ_i, X_{key} is the set of key state variables which significantly affects the eigenvalue, while X_{VSC}, X_{net} are the set of state variables belonging to the VSC and network respectively. Ordering the state variables in descending rank of participation factor, the key state variables are selected (in this work) as the top-ranked state variables with participation factors of at least 1/10 relative to the highest value. A list of key state variables is therefore obtained per eigenvalue. The key eigenvalues are those that have key state variables belonging to both the VSC and the network.

3.2. Matching the key eigenvalues

Having identified the key eigenvalues which involve VSC and network states from the different models being compared, the next step is to identify how accurately the eigenvalues are reproduced when using a reduced order model (i.e. either a steady state or a hybrid network representation). To do this, it is necessary to try and match eigenvalues from the reduced-order models to those obtained from linear analysis of the full dynamic model (where all network lines have ODE

representation). Reducing the order of the dynamic modelling means that some key eigenvalues may no longer be captured (as their key states may be removed from the model). If all key eigenvalues can be found in the reduced order model, then the accuracy of their placement in the complex plane can be assessed.

Differing from previous research on this topic, this section adopts a systematic comparison procedure in order to identify similar eigenvalues from the reduced order and full dynamic models using Spearman's correlation coefficient. The correlation coefficient is used to quantify the similarity between the key state variable lists (ranked by participation factor) for each key eigenvalue (from the full dynamic model) and possible candidate matches (from the reduced order models).

Consider the eigenvalues obtained from a reduced order model λ_{red}, and those from the full dynamic model λ_{full}. Each eigenvalue has a key state variables list, ranked by participation factor. The order of the key state variables list from the full dynamic model and the reduced model are R and S respectively. The corresponding Spearman's correlation of the key state variables ranking from the models is represented as (6).

$$\rho = \frac{cov(R,S)}{\sigma_R \sigma_S} \tag{6}$$

In (6), R, S denotes the rank of the corresponding key state variables; $cov(R,S)$ represents the covariance of the rank state variables; while σ_R σ_s represent the standard deviations of the corresponding rank state variables.

The Spearman's correlation coefficient ρ varies between -1 to $+1$. When the value is close to $+1$, the two ranked lists of key state variables (for the full dynamic and reduced order model eigenvalues) are monotonic with a positive linear rank correlation. That means the eigenvalues have matching rank orders of state variables and the eigenvalues can be considered to be similar (and representative of the same dynamic behavior). If the correlation value ρ is close to zero, it means that the lists of eigenvalue participating states are not ranked similarly and it is unlikely that the eigenvalues are a match. Given that the full dynamic model includes the full dynamic details of the power system, it presents the largest number of state variables. Therefore, per eigenvalue λ_{red} obtained from the steady-state or the hybrid model, the Spearman's correlation coefficient ρ is calculated between the key state variables lists from λ_{red}, and every eigenvalue λ_{full} from the full dynamic model. In this work, the eigenvalue from the reduced order model which has the highest correlation value exceeding 0.8 will be deemed to match the full dynamic model key eigenvalue.

The following section describes an example of matching eigenvalues from the full dynamic and reduced-order models using the proposed comparison method. Fig. 2 shows an example of the distribution of eigenvalues obtained from the full dynamic and reduced-order models. The modes from full dynamic model are colored blue and the eigenvalues from reduced order model are colored red. Taking eigenvalue A from the full model as an example, the participation factor analysis shows that the state variables related to the VSC and to the current passing through line 2-30 participate most in the mode. Referring to Fig. 2, there are eight potential modes from the reduced-order model that are located around eigenvalue A (shown in the figure as surrounded by a dashed line). Among those eigenvalues, mode B' is closest to mode A (with respect to Euclidean distance in the eigenvalue plane). However, based on the results of participation factor analysis, the state variables from the VSC and G38 participate strongly in mode B'. Although mode A' is further from mode A, it is dominated by the state variables belonging to the line 2-30 and the VSC which matches the participation value distribution of the target mode A. Following the proposed comparison method, mode A' therefore matches eigenvalue A.

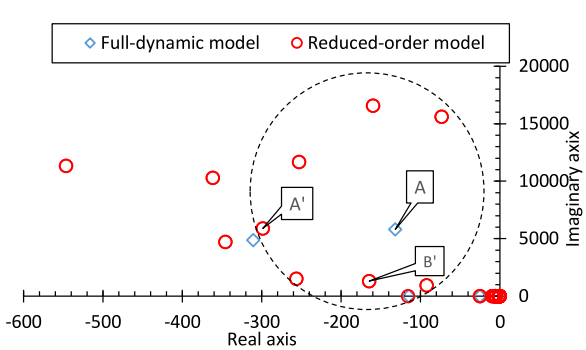

Fig. 2. Example of the distribution of eigenvalues obtained from the full- and reduced-order models.

3.3. Quantifying the difference

In the ideal case, and considering results from full dynamic model as standard, all of the key eigenvalues identified from the full model should have a corresponding matching eigenvalue from the steady-state or hybrid model. With reduced order modelling, and the removal of key network dynamic states, this is not always the case. Calculating the error between the key eigenvalues obtained from different models should only occur once all key eigenvalues are represented in the reduced order model. Otherwise, a cumulative damping ratio error may produce a misleading quantitative determination of the difference between models.

Therefore, in this paper, the key eigenvalues identified from full models are divided into a *matched* group and an *unmatched* group. The matched group contains all key eigenvalues for which a match has been identified from the reduced order model. This paper adopts the ratio of the number of matched eigenvalues to the total number of key eigenvalues to quantify the suitability of the reduced order model.

When all key eigenvalue matches have been identified, the cumulative damping ratio error to establish the difference between the full and reduced order models is adopted. The calculation of the cumulative damping ratio error between the different models is presented in (7).

$$\varepsilon_\xi = \sum_{\lambda_{full},\lambda_{red}} \frac{\left|\left(\xi(\lambda_{full}) - \xi(\lambda_{red})\right)\right|}{\xi(\lambda_{full})} \tag{7}$$

In (7), λ_{full}, λ_{red} are the matched eigenvalues denoting the eigenvalues from the full and reduced order models respectively, while ξ is the eigenvalue damping ratio. Error is calculated with respect to damping ratio as it is typically considered to be an important index for small-signal stability analysis. The damping ratio represents the rate of decay of amplitudes of oscillation associated with the mode. In a real-world power system, it is derisible to restore a steady-state quickly after a disturbance. Therefore, accuracy in preserving the damping ratio is desirable. However, if preferred, the use of damping ratio could be changed for any index of interest related to small-disturbance stability. For example, the real part of the eigenvalue or frequency of the mode could be used to quantify the difference between the models.

3.4. Summary of Application Procedure

This section will summarize the application procedure of the proposed methodology, which is as follows.

Step 1: Develop the full dynamic model and steady-state or hybrid model based on the modelling method illustrated in Section II.

Step 2: Select the key eigenvalues from the different models according to (5).

Step 3: Identify the similar eigenvalue matches according to (6). The eigenvalue match with the highest Spearman's correlation coefficient value that exceeds 0.8 will be deemed a similar matched eigenvalue.

Step 4: Check if all the key eigenvalues from the full model have a corresponding match from the reduced order model. If so, then calculate the damping ratio error with (7). Otherwise, calculate the matched

proportion over all key eigenvalues.

4. Numeric Results

The IEEE 39 bus with modifications is adopted here to demonstrate the proposed methodology. This section uses three different cases:

1 *SGs are replaced with VSCs*. The SG at each generator bus is replaced (one at a time) by a VSC with a cascaded GFL control scheme. The VSC has the same capacity as the replaced SG and operates with P-Vac outer control [12]. Different reduced order models (with steady-state and hybrid network modelling) will be compared with the full dynamic model across these different VSC-SG replacement locations to establish and explore the error seen between the models.
2 *Loads replaced with VSCs*. Similar to Case 1, each load in the system will be replaced (one at a time) by a VSC with the same capacity operating with P-Q control [12] . In a real-world power system, it is uncommon to have a VSC operate with P-Vac control in rectifier mode. It should be noted that this paper focuses on the impact of the VSC operating mode (rectifying or inverting) rather than different grid-following control schemes in the hybrid model. Therefore, each load in the system is replaced by a VSC operating with P-Q control.
3 *SGs replaced with GFMs*. Finally, the impact of using VSM controlled GFMs will be investigated by comparing different network model orders at key SG locations.

4.1. Case 1 - SGs are replaced with VSCs

The first case presented involves the substitution of each SG with a GFL-VSC. Firstly, the results between steady-state and full dynamic models are summarized in Table 1, after applying the outlined methodology to match key eigenvalues.

The percentage of matched key eigenvalues for each VSC replacement location is shown in Fig. 3 plotted against the short circuit ratio (SCR) for each location. The SCR value is calculated at the location of the original SG which is replaced by the VSC. The trend line in Fig. 3 shows that there is strong linear positive correlation between SCR values and proportion of matched key eigenvalues. This indicates that with a higher SCR, the VSC is less likely to interact with the network. This results in a greater number of matched eigenvalues even with the steady-state model. Therefore, smaller regions of the network require dynamic modelling in order to capture all key eigenvalues and improve the accuracy of the small signal analysis results. This finding aligns with the conclusions from previous work [7] whereby a higher SCR indicates a lower total sum of errors between steady-state and full dynamic models.

These results have compared the full dynamic model with the steady-state model. It can be seen that in all cases, key eigenvalues remain unmatched and the steady-state network representation is not sufficient. Therefore, hybrid modelling is investigated to first establish the network region which must be dynamic to match all key eigenvalues, and subsequently to see how the error in those matched eigenvalues varies with increasing dynamic network representation. However, if there are changes in the network conditions, this may increase the SCR seen by the VSC, and a lower-order, hybrid model would be appropriate. For example, with additional network reinforcement, the conventional steady-state network model with algebraic equations may be sufficient to capture those oscillations caused by the network-VSC interactions.

Table 1
COMPARISON OF STEADY-STATE MODEL AND FULL DYNAMIC MODEL FOR SG REPLACED BY VSC CASE.

Generator Bus	*Number of eigenvalues*	*Matched*	*Unmatched*
30	6	5	1
32	5	4	1
33	6	4	2
34	8	5	3
35	7	4	3
36	6	4	2
37	8	5	3
38	11	4	7
39	5	3	2

The following terminology is used to refer to hybrid models of different order. Within the *Hybrid-1* model, the buses and line that are adjacent to the VSC are modelled with ODEs. Within the *Hybrid-2* model, the ODE-represented region is expanded to include the lines and buses adjacent to those modelled dynamically in *Hybrid-1*. This continues for *Hybrid-3* and so on, expanding the ODE-represented region, until the full dynamic model is achieved. This is illustrated taking the VSC replacement of the SG at bus 30 as an example, shown in Fig. 4. The details of the first two hybrid-level models are:

- *Hybrid-1*: buses 2 and 30; lines 2-30, 2-1, 2-3, 2-25. These are designated with red color, surrounded by a dashed line.
- *Hybrid-2*: same as above, and also including buses 1, 3, 25 and 37; lines 1-39, 3-4, 3-18, 25-37 and 25-26; loads at bus 3 and bus 25. These are designated with blue color, surrounded by dotted line.

The increase in modelling burden caused by different hybrid model orders is shown taking the VSC connected to bus 30 as an example. The number of state variables in the different hybrid-level models are shown in Table 2. The number of state variables in the hybrid models increases exponentially as the hybrid degree increases from *Hybrid-1* to *Hybrid-5*.

Fig. 5 shows the hybrid modelling order necessary to ensure that all key eigenvalues are matched, plotted against the SCR at the different locations. This plot is complementary to Fig. 3 (which showed the proportion of matched key eigenvalues with steady-state network modelling). The strong negative correlation (R^2=0.9063) in Fig. 5 indicates that higher order hybrid models are needed to capture the VSC-network interactions when VSCs are located in low SCR regions.

Once all key eigenvalues are matched, hybrid model order can still be increased further to improve the result accuracy with respect to eigenvalue placement. The comparisons of different order hybrid models with the full dynamic model are shown in Table 3, using bus 30 as an example. After all eigenvalues are matched (which happens with *Hybrid-1*), the cumulative damping ratio error, calculated by (7), reduces from 0.5405 to 0.4336 as the model order increases to *Hybrid-5*. Considering the acceptable relative error (0.01) set in methodology, the relative reduction of the damping ratio error is 0.1978, which is significant.

In this paper, an eigenvalue from the hybrid model can only match with one unique mode from the full model. This fact, along with the threshold setting in the eigenvalue comparison methodology developed, could affect the results obtained. It should be noted that although the details about the number of key eigenvalues identified may be influenced by these factors, the conclusions about the relationship between the SCR and network area requiring dynamic representation remains the same. The developed methodology is applied to different VSC control schemes and considering different VSC operation modes (always using the same eigenvalue matching criteria) to make sure that the results are comparable between sections.

Fig. 6 shows the damping ratio error with increasing hybrid model order after all the key eigenvalues have been matched for VSC replacements at bus 30 and bus 33. Similar plots can be produced for other locations. At bus 30, all key eigenvalues are matched using *Hybrid-1*, while at bus 33, *Hybrid-2* is required to match all key eigenvalues. The trend seen in Fig. 6 for both locations is similar, with the error following a logarithmic reduction with increasing hybrid model order. For bus 33, comparing *Hybrid-3* to *Hybrid-2*, the error decreases from 1.3834 to 0.8908, a reduction of 35.61%. However, the error only reduces 10.70% from 0.7675 to 0.6854 when increasing the model order from *Hybrid-4* to *Hybrid-5*. This is due to the VSC having a greater likelihood of

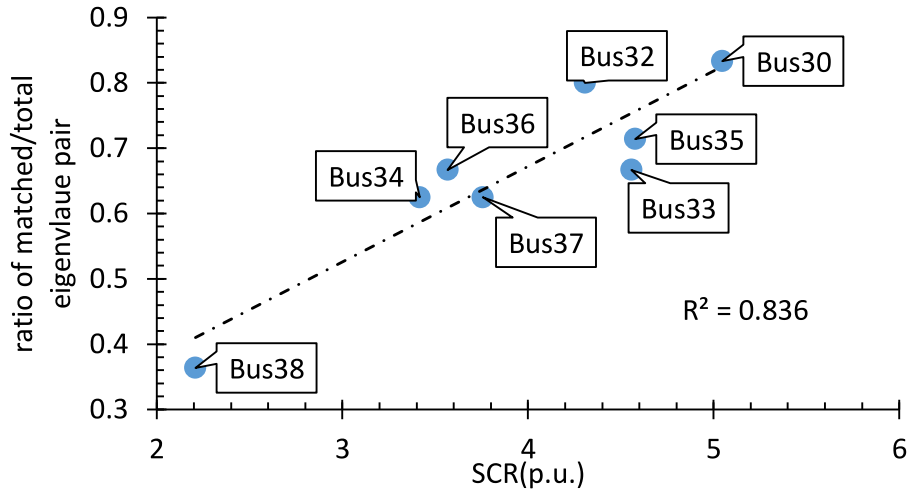

Fig. 3. Matched proportion with respect to SCR at different locations.

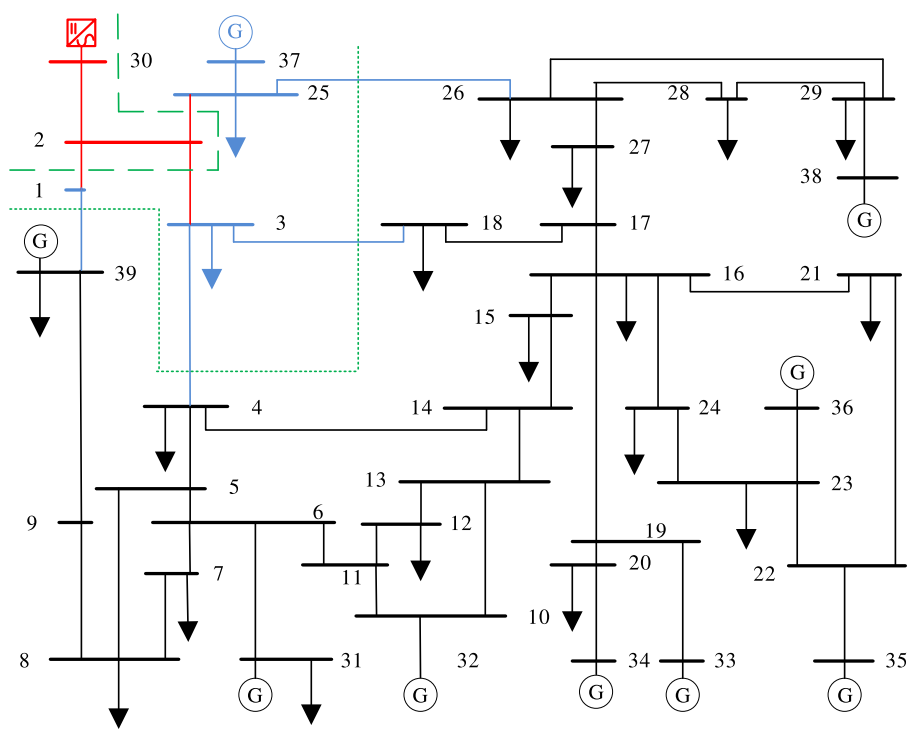

Fig. 4. Hybrid-1 and Hybrid-2 ODE-network regions for VSC at bus 30.

Table 2
NUMBER OF STATE VARIABLES IN DIFFERENT IEEE 39 MODELS FOR VSC CONNECTED BUS 30 CASE.

Model elements	Full Dynamic	Steady-state	Hybrid model order 1	2	3	4	5
Converter	10	10	10	10	10	10	10
Network	206	0	12	34	64	104	144
Generators	61	61	61	61	61	61	61
Overall	**277**	**71**	**83**	**105**	**135**	**175**	**215**

interacting with the immediately adjacent network and therefore there are diminishing gains to expanding the dynamic area. Hence, the balance between the degree of accuracy and the dimension of the system matrix should be considered.

4.2. *Case 2 – Loads are replaced with VSCs*

The results from Case 1 have shown the impact of network dynamic modelling detail on small signal analysis result accuracy when integrating VSCs operating as inverters into the system. Now, in Case 2, the loads in the IEEE 39 bus system will be replaced by GFL-VSCs. The VSCs will have the same operational capacity as the load they replace and operate as a rectifier with a standard P-Q control scheme. The differences between steady-state and full dynamic models for VSC replacements at each location are summarized in Table 4.

The results within Table 4 are arranged in SCR increasing order. Table 4 shows that for almost all locations (12 out of 16 load buses), all key eigenvalues are matched when using a steady-state network representation. This is because when the VSC operates as a rectifier, it is less likely to interact with the network [17]. The number of key eigenvalues is reduced and steady-state network representation is generally

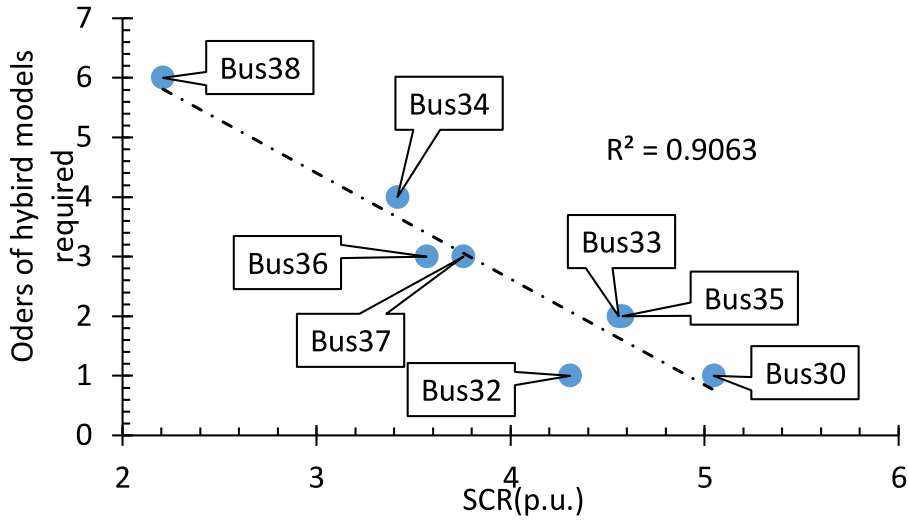

Fig. 5. Hybrid modelling order required to guarantee all key eigenvalues matched with respect to SCR at different locations.

Table 3
Damping ratio error FOR BUS 30

Hybrid model order	1	2	3	4	5
Damping ratio error	0.5405	0.4546	0.4459	0.4355	0.4336

appropriate. In general, when the VSC operates as a load, the network requiring ODE representation is reduced.

However, network dynamics cannot be neglected in all cases. At buses 8, 12, 28 and 29 higher order (hybrid) modelling is needed. These locations again correspond with low SCR regions of the network. For example, the SCR at bus 12 is 4.95, which is lower than the other load buses and hence only 5 out of 10 key eigenvalues are matched. It should also be noted that the lowest SCR location also corresponds with the highest number of key eigenvalues. Increasing hybrid model orders for these locations results in more matched eigenvalues and reducing errors with similar trends to those shown previously for SG-replacement in Case 1.

4.3. Case 3 – SGs are replaced with GFMs

In this final case, the SGs at the investigated buses are replaced by a GFM with the same operational capacity as the SG. The GFM architecture is that of Fig. 1 in which an inner current controller is included for the purposes of current limitation. The results are displayed for the GFM at buses 30 and 38 since these have been seen to be the strongest and weakest buses, respectively. The virtual inertia constant and damping coefficient are set to 4 s and 10 p.u. torque/p.u. speed deviation, respectively. The virtual inductive reactance is set at 0.2 p.u. and the inner current controller and voltage magnitude controller have the same tunings as for the GFLs used previously.

Table 5 reports the differences between the steady-state and full dynamic models for GFMs at the buses of interest. The number of key eigenvalues identified is higher than in Case 1 in which the SGs were replaced by VSCs with GFL control. As an example, for bus 30 in Case 1 there were six key eigenvalues, whereas eight are identified for this case. It was also found that it takes *Hybird-6* and *Hybird-8* for bus 30 and bus 38 scenarios to match all eigenvalues, respectively. This is also higher than Case 1 where only *Hybird-1* was needed for the bus 30, and *Hybird-6* for bus 38.

To provide more information about the key eigenvalues, the results for bus 30 are discussed in more detail. At hybrid level 5, one unmatched eigenvalue remains whose characteristics are shown in Table 6.

The remaining unmatched eigenvalue is a high frequency mode, and it is clear from the dominant states that this is an electrical resonant mode. Small participations from the VSC RL output filter flag this as a key eigenvalue and similar modes are present in prior hybrid levels. It might be that eigenvalues like this one are largely irrelevant for dynamics associated with the GFM. However, the assessment within this

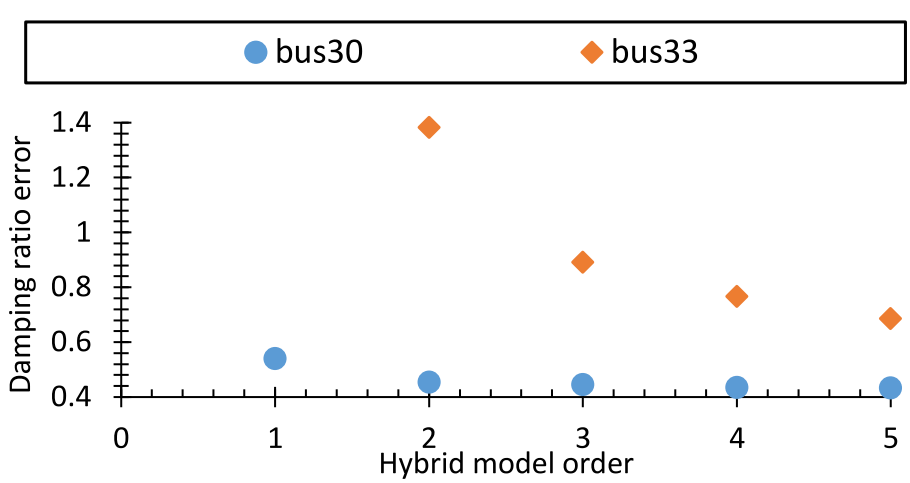

Fig. 6. The damping ratio error with respect to the hybrid model order.

Table 4
COMPARISON OF STEADY-STATE MODEL AND FULL DYNAMIC MODEL FOR LOAD REPLACED BY VSC CASE

Load Bus	*No. key eigenvalues*	*Matched*	*Unmatched*	*SCR*
12	10	5	5	4.954
28	4	3	1	5.640
29	4	3	1	7.583
27	3	3	0	8.176
26	2	2	0	8.511
20	4	4	0	8.650
7	2	2	0	9.922
21	2	2	0	10.125
8	3	2	1	10.278
15	2	2	0	10.456
18	1	1	0	10.532
25	1	1	0	10.550
23	1	1	0	10.580
4	3	3	0	11.726
3	2	2	0	12.157
16	1	1	0	14.952
16	1	1	0	14.952

Table 5
COMPARISON OF STEADY-STATE MODEL AND FULL DYNAMIC MODEL FOR SG REPLACED BY GFM CASE

Generator Bus	Number of key eigenvalues	Matched	Unmatched
30 (highest SCR)	8	2	6
38 (lowest SCR)	14	3	11

Table 6
BUS 30 FINAL UNMATCHED EIGENVALUE CHARACTERISTICS.

	Eigenvalue	Dominant states
Key Eigenvalue	-3.3043e+02 + 4.7696e+03i	Bus voltages: 2, 26, 28 Branch currents: 1-2, 26-28

paper is not based on the significance of the eigenvalues with respect to potential instability. Therefore, these modes are not neglected in this study. The authors believe the identification of electrical resonant key modes in the GFM case (and therefore a greater number of key modes being associated with GFMs compared to GFLs) may stem from small differences in eigenvalue participation leading to different key eigenvalue identification due to the selected threshold values. As it stands, the procedure proposed in this work can be considered a heuristic. Future work will focus on optimizing the process, considering key information such as the consequential impact on stability from the modes of interest, as well as identifying whether an objectively optimal approach for eigenvalue matching exists.

The same analysis is performed for GFMs without an inner current loop and without a virtual inductance. All other elements remain the same. The low bandwidth of the controller leads to no interactions between the GFM controls and the network dynamics meaning an algebraic representation is sufficient to match all eigenvalues. In this case, only eigenvalues where GFM control states participate highly were considered.

5. Conclusion

This paper develops a methodology to determine the network region that needs to be modelled dynamically to capture small signal interactions between converters and network elements. The method introduces correlation based analysis of participation factors to identify matching eigenvalues, providing a quantitative comparison in terms of small signal stability assessment for AC networks modeled with different levels of detail. The assessment is performed for networks ranging from full steady-state representation (i.e. using algebraic equations) to full dynamic representation (using ODEs). Between the two extremes, hybrid models (i.e. a mix of steady-state and ODE representation) are used, increasing the size of the region represented dynamically as the hybrid model order increases. Case studies with VSCs operating in GFL, GFM, inverter and rectifier control mode are investigated, highlighting the need to model parts of the network dynamically in order to capture key eigenvalues, especially when SCR is low. With the dynamic area of a hybrid model expanding, all matched eigenvalues are expected to be found. After that, the eigenvalue damping ratio error can be used to describe the accuracy of different models compared with a fully dynamic model.

Results from a modified version of IEEE 39 bus network show that in general for the GFL case, converters can interact with the network and some level of hybrid model order is needed to capture all the key eigenvalues. The order of hybrid model needed rises as the SCR decreases. After all key eigenvalues are matched, increasing the hybrid model order reduces the damping error of the eigenvalues in a logarithmic way. This behavior is similar but less pronounced with VSCs operating in rectifier mode when eigenvalues are generally more easily matched either with a steady-state or a lower hybrid order model, apart from particular locations with low SCR. When the VSC operates with GFM control, there is an increase in the network portion that requires hybrid modelling to capture all relevant eigenvalues. However, if a GFM architecture without an inner current controller is used, the steady-state model can likely capture eigenvalues of interest where the converter control states participate due to the low bandwidth of the control.

CRediT authorship contribution statement

Youhong Chen: Writing – original draft, Software, Validation, Conceptualization, Formal analysis. **Luke Benedetti:** Writing – original draft, Software, Validation, Conceptualization. **Robin Preece:** Writing – review & editing, Supervision, Conceptualization. **Panagiotis N. Papadopoulos:** Writing – review & editing, Supervision, Conceptualization. **Mike Barnes:** Writing – review & editing, Supervision, Conceptualization. **Agustí Egea-Àlvarez:** Writing – review & editing, Supervision, Conceptualization.

Declaration of Competing Interest

The authors declare that they have no known competing financial interests or personal relationships that could have appeared to influence the work reported in this paper.

Acknowledgments

Financial support is acknowledged from EPSRC through the Power Networks Centre for Doctoral Training (EP/L016141/1), an EPSRC Student Excellence Award Studentship, and a UKRI Future Leaders Fellowship (MR/S034420/1). All results can be fully reproduced using the methods and data described in this paper and provided references.

References

[1] P.S. Kundur, *Power System Stability and Control*, Third, McGraw-Hill, New York, 2017.
[2] M. Paolone, et al., Fundamentals of Power Systems Modelling in the Presence of Converter-Interfaced Generation, in: 21st Power Systems Computation Conference 189, 2020.
[3] N. Hatziargyriou et al., "Stability definitions and characterization of dynamic behavior in systems with high penetration of power electronic interfaced technologies," 2020.
[4] X. Wang, F. Blaabjerg, Harmonic Stability in Power Electronic-Based Power Systems: Concept, Modeling, and Analysis, IEEE Trans. Smart Grid 10 (3) (2019) 2858–2870.
[5] C. Karawita, U.D. Annakkage, Multi-infeed HVDC interaction studies using small-signal stability assessment, IEEE Trans. Power Deliv. 24 (2) (2009) 910–918.
[6] C. Karawita, U.D. Annakkage, A hybrid network model for small signal stability analysis of power systems, IEEE Trans. Power Syst. 25 (1) (Feb. 2010) 443–451.

[7] G. Grdenić, M. Delimar, J. Beerten, Assessment of AC network modeling impact on small-signal stability of AC systems with VSC HVDC converters, Int. J. Electr. Power Energy Syst. 119 (December 2019), 105897, 2020.
[8] D. Groß, M. Colombino, J.-S. Brouillon, F. Dorfler, The Effect of Transmission-Line Dynamics on Grid-Forming Dispatchable Virtual Oscillator Control, IEEE Trans. Control Netw. Syst. 6 (3) (2019) 1148–1160, https://doi.org/10.1109/TCNS.2019.2921347.
[9] S. D. Arco and J. A. Suul, "Virtual Synchronous Machines – Classification of Implementations and Analysis of Equivalence to Droop Controllers for Microgrids," 2013.
[10] P. Peter, W. Sauer, Power System Dynamics and Stability, M. A., The University of Illinois, Urbana, 1997.
[11] IEEE PES, "IEEE Recommended Practice for Excitation System Models for Power System Stability Studies," 2016.
[12] W. Wang, Operation, Control and Stability Analysis of Multi-Terminal VSC-HVDC Systems, Manchester, UK Univ. Manchester 2015 (2015).
[13] A. Egea-Alvarez, A. Junyent-Ferré, O. Gomis-Bellmunt, Active and Reactive Power Control of Grid Connected Distributed Generation Systems, Modeling and Control of Sustainable Power Systems (2012) 47–81.
[14] S. D'Arco, J.A. Suul, O.B. Fosso, Control system tuning and stability analysis of Virtual Synchronous Machines, IEEE Energy Conversion Congress and Exposition (2013) 2664–2671.
[15] S. Drarco, G. Guidi, J.A. Suul, Operation of a Modular Multilevel Converter Controlled as a Virtual Synchronous Machine, in: 2018 International Power Electronics Conference 2018, IPEC-Niigata - ECCE Asia, Oct. 2018, pp. 782–789.
[16] T. Qoria, C. Li, K. Oue, F. Gruson, F. Colas, X. Guillaud, Direct AC voltage control for grid-forming inverters, J. Power Electron. 20 (1) (2020) 198–211.
[17] J.Z. Zhou, H. Ding, S. Fan, Y. Zhang, A.M. Gole, Impact of Short-Circuit Ratio and Phase-Locked-Loop Parameters on the Small-Signal Behavior of a VSC-HVDC Converter, IEEE Trans. Power Deliv. 29 (5) (2014) 2287–2296.